Supplementary Material

Fabrication, Crystal Structures, Catalytic and Anti-wear Performance of 3D Zinc(II) and Cadmium(II) Coordination Polymers Based on a Tetracarboxylate Ligand

Zhenghua Zhao [1], Qin Zhang [1], Yufeng Liu [1], Jinzhong Gu [2,*], Zifa Shi [2,*]

[1] Petrochina Lanzhou Lube Oil R&D Institute, Lanzhou, 730060, China; zhaozhenghua_rhy@petrochina.com.cn (Z.Z.); zhangqinlz_rhy@petrochina.com.cn (Q.Z.); liuyufeng_rhy@petrochina.com.cn (Y.L.)

2 State Key Laboratory of Applied Organic Chemistry and College of Chemistry and Chemical Engineering, Lanzhou University, Lanzhou, 730000, China

* Correspondence: gujzh@lzu.edu.cn (J.G.), shizf@lzu.edu.cn (Z.S); Tel.: +86-931-8915196 (J.G.), +86-931-8912500 (Z.S.)

Contents

Figure S1. FT-IR spectra of compounds **1** and **2**. S2
Figure S2. PXRD patterns of compounds **1** and **2** at room temperature. S2
Figure S3. The coordination modes of $dppa^{4-}$ linkers in this work and previously reported works. S3
Figure S4. Example of the integration in the ^1H NMR spectrum of the reaction mixture for the determination of Knoevenagel condensation product (conditions of Table 2, Entry 6). S3
Figure S5. Example of the integration in the ^1H NMR spectrum of the reaction mixture for the determination of Knoevenagel condensation product (conditions of Table 2, Entry 8). S4
Figure S6. Accumulation of 2-benzylidenemalononitrile vs. time in the Knoevenagel condensation of benzaldehyde with malononitrile catalysed by **1** (blue dotted line refers to the reaction after removal of the catalyst after 10 min reaction time; see text for details). Reaction conditions are those of Table 2, entries 1−6. ..... S4
Figure S7. Catalyst recycling experiments in the Knoevenagel condensation of benzaldehyde with malononitrile catalysed by **1**. Reaction conditions are those of Table 2, entry 7. ..... S5
Figure S8. PXRD patterns for **1** and **2**: simulated (red), before (black) and after (blue) catalysis. S5
Figure S9. Plausible mechanism for the Knoevenagel condensation reaction catalyzed by **1**. S5
Figure S10. Fluorescence images of the powder of 1 under dark-field (a) and bright-field (b); fluorescence images of **1/PAO10** under dark-field (c) and bright-field (d). S6
Figure S11. PXRD patterns for **1** [simulated (red), powder (black) and powder from **1/PAO10** (blue)]. S6
Table S1. Reported coordination polymers with $dppa^{4-}$ ligand. S7
Table S2. Selected bond lengths (Å) and bond angles (º) for compounds **1** and **2**. S8
Table S3. Hydrogen bond lengths (Å) and angles (º) of compound **2**. S8
Table S4 Substrate scope for Zn-catalyzed the Knoevenagel condensation reaction of substituted benzaldehydes with malononitrile [a] S9
Table S5. Comparison of various catalysts for the Knoevenagel condensation reaction between benzaldehyde and propanedinitrile. S10

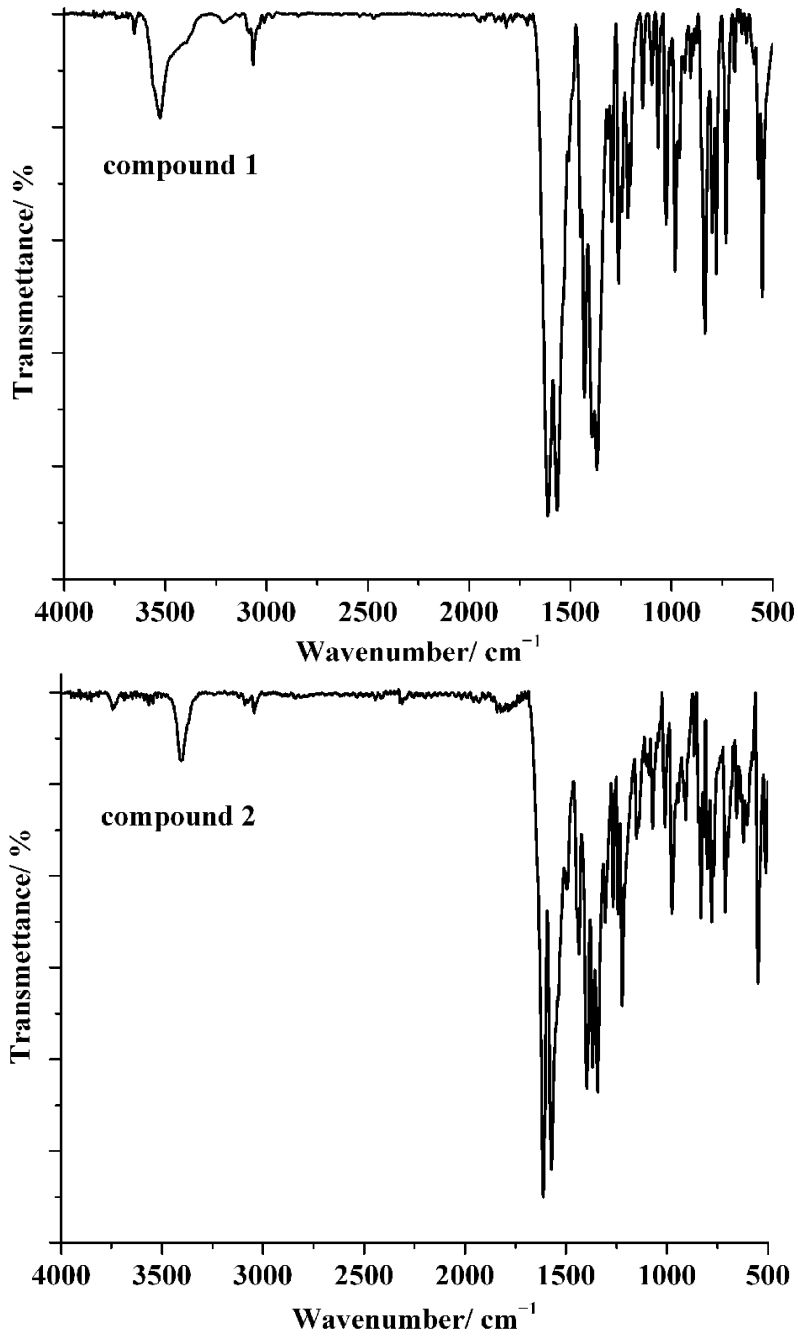

Figure S1. FT-IR spectra of compounds **1** and **2**.

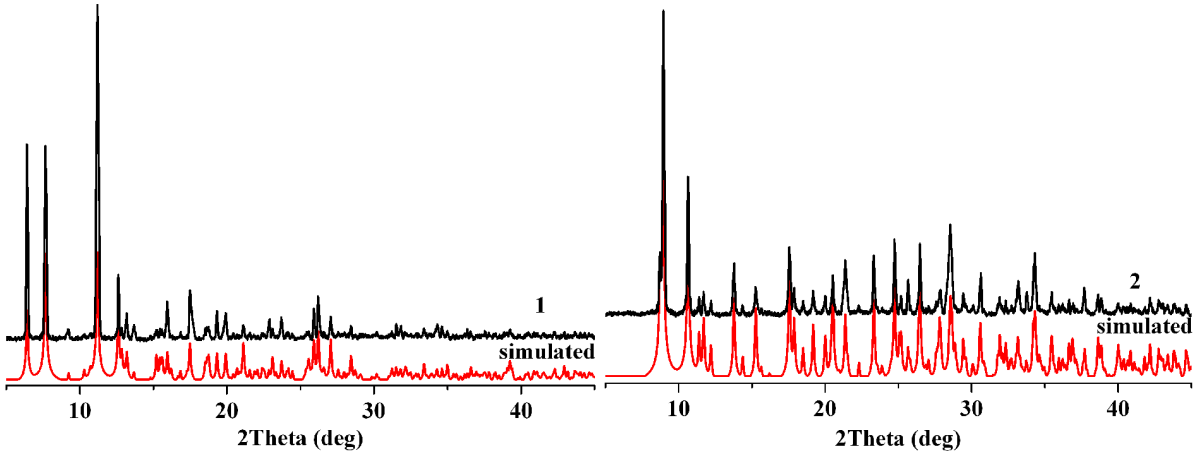

Figure S2. PXRD patterns of compounds **1** and **2** at room temperature.

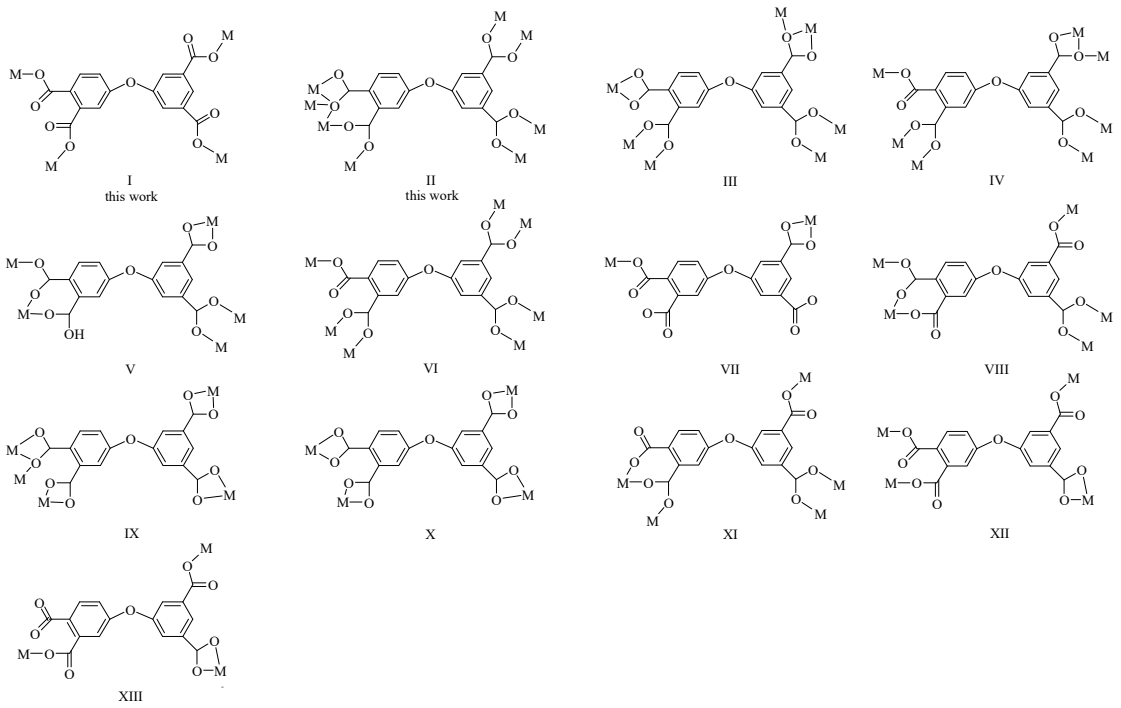

Figure S3. The coordination modes of $dppa^{4-}$ linkers in this work and previously reported works.

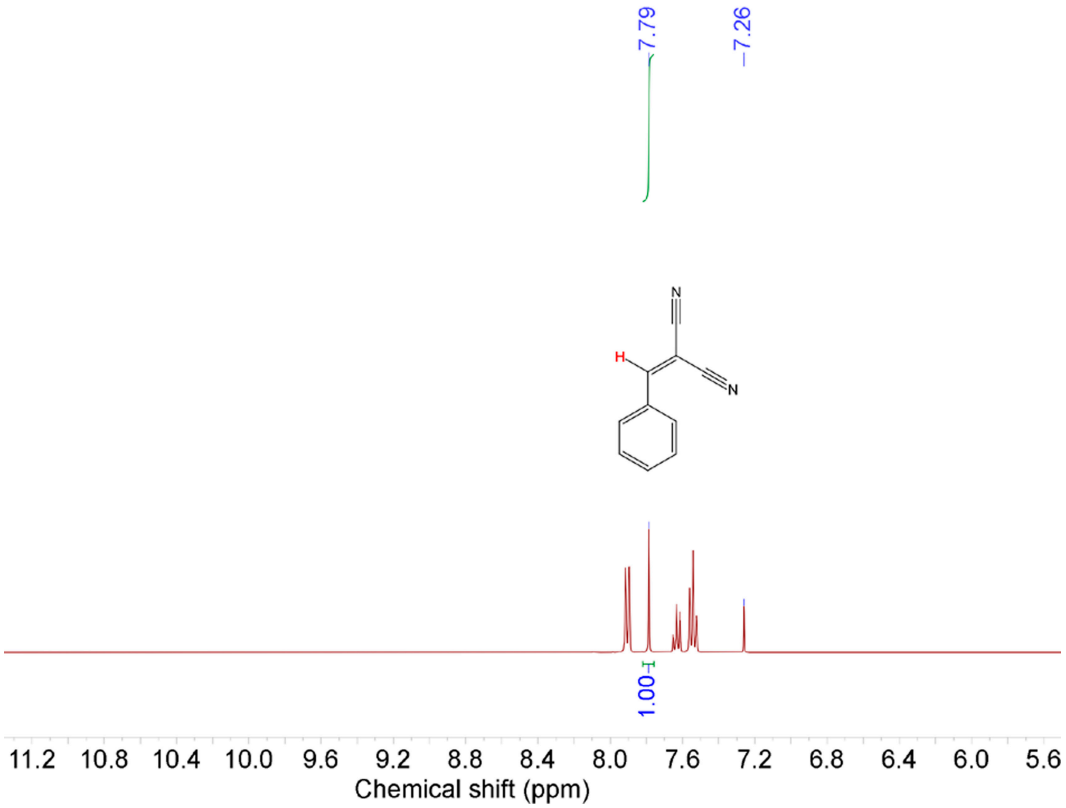

Figure S4. Example of the integration in the ^{1}H NMR spectrum of the reaction mixture for the determination of Knoevenagel condensation product (conditions of Table 2, Entry 6).

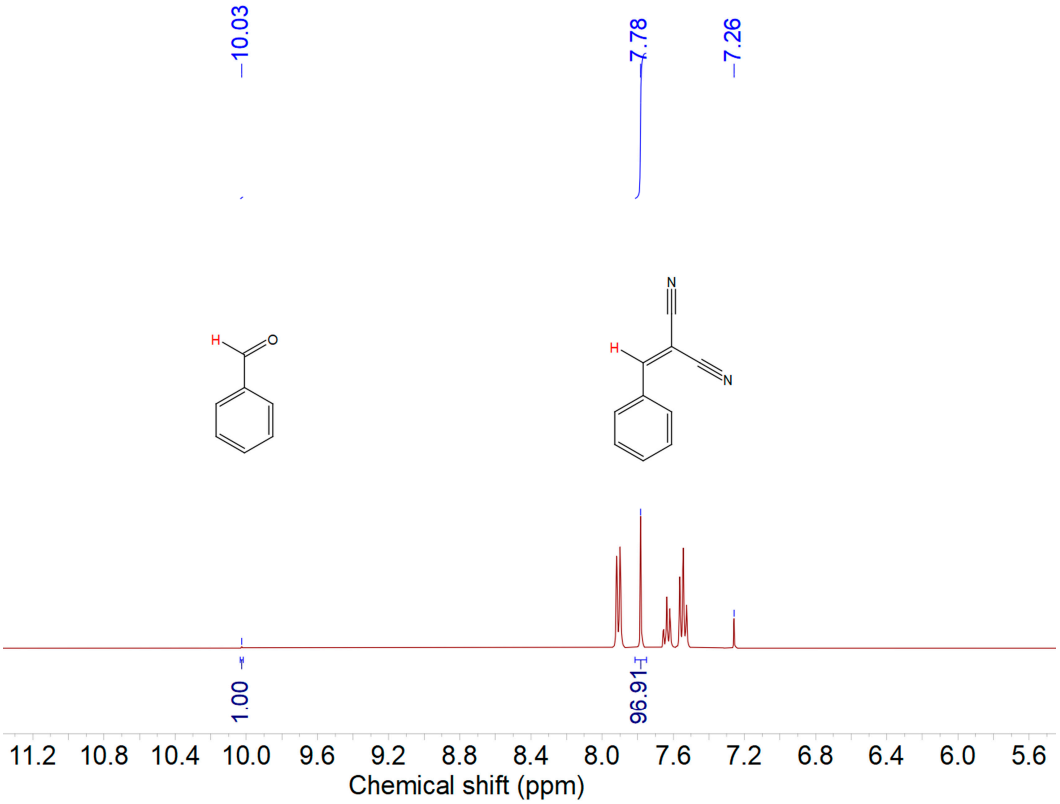

Figure S5. Example of the integration in the ^{1}H NMR spectrum of the reaction mixture for the determination of Knoevenagel condensation product (conditions of Table 2, Entry 8).

Product yield calculation in the Knoevenagel condensation reaction. The C(=O)*H* signal of benzaldehyde (substrate) appears at δ 10.03 ppm, while 2-benzylidenemalononitrile (product) shows a characteristic signal at δ 7.78 ppm.

Total integration of both signals: unreacted benzaldehyde + 2-benzylidenemalononitrile = 1.00 + 96.91 = 97.91.

Percentage of the unreacted substrate: 1/97.91 = 1.02%

Conversion of benzaldehyde = yield of 2-benzylidenemalononitrile = 100 − 1.02 = 98.98%.

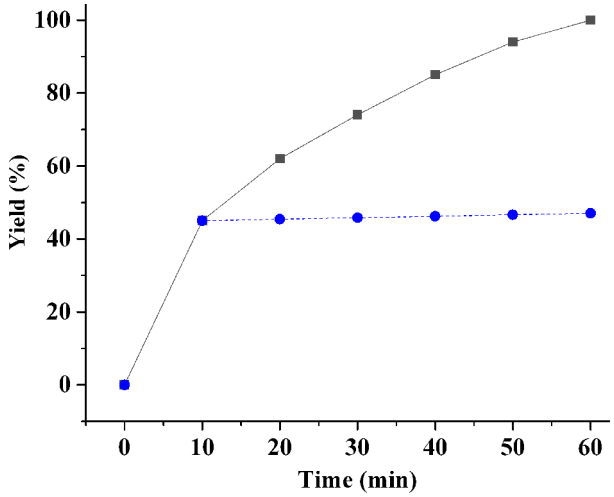

Figure S6. Accumulation of 2-benzylidenemalononitrile vs. time in the Knoevenagel condensation of benzaldehyde with malononitrile catalysed by **1** (blue dotted line refers to the reaction after removal of the catalyst after 10 min reaction time; see text for details). Reaction conditions are those of Table 2, entries 1−6.

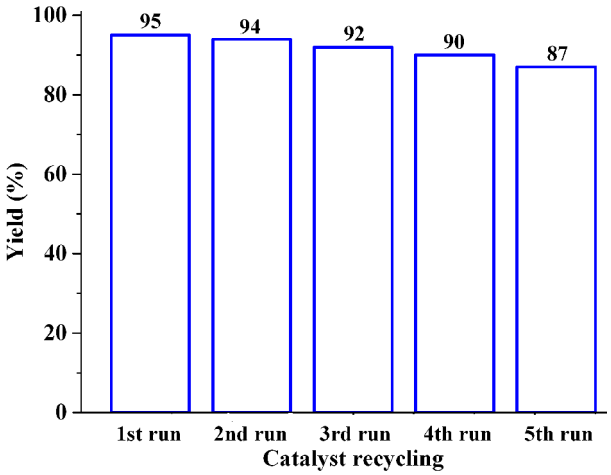

Figure S7. Catalyst recycling experiments in the Knoevenagel condensation of benzaldehyde with malononitrile catalysed by **1**. Reaction conditions are those of Table 2, entry 7.

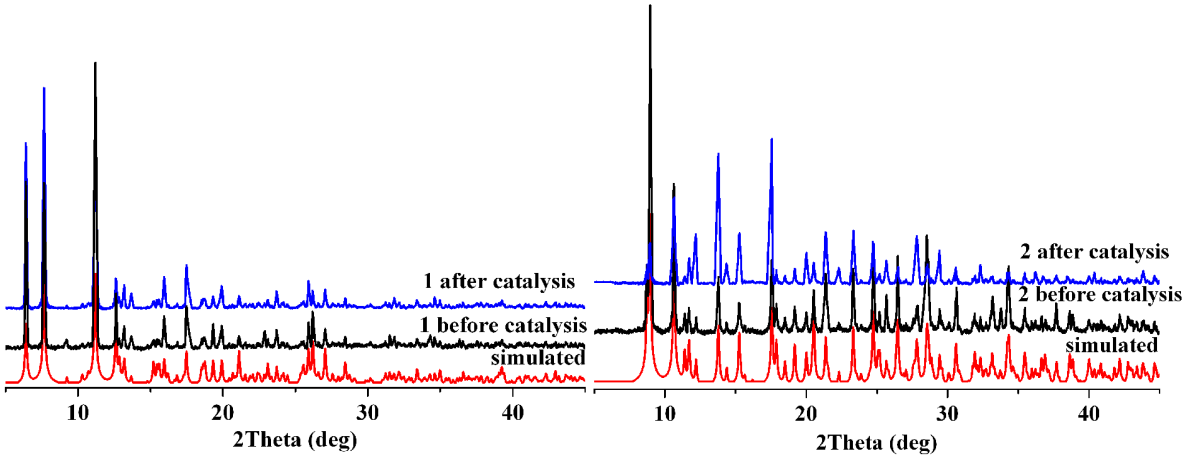

Figure S8. PXRD patterns for **1** and **2**: simulated (red), before (black) and after (blue) catalysis.

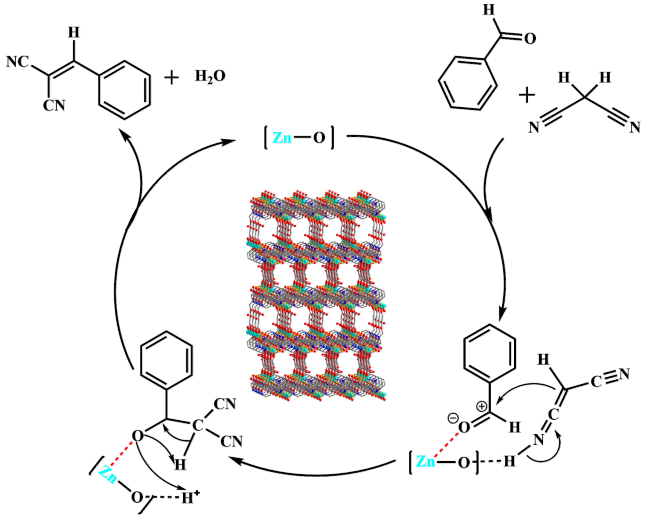

Figure S9. Plausible mechanism for the Knoevenagel condensation reaction catalyzed by **1**.

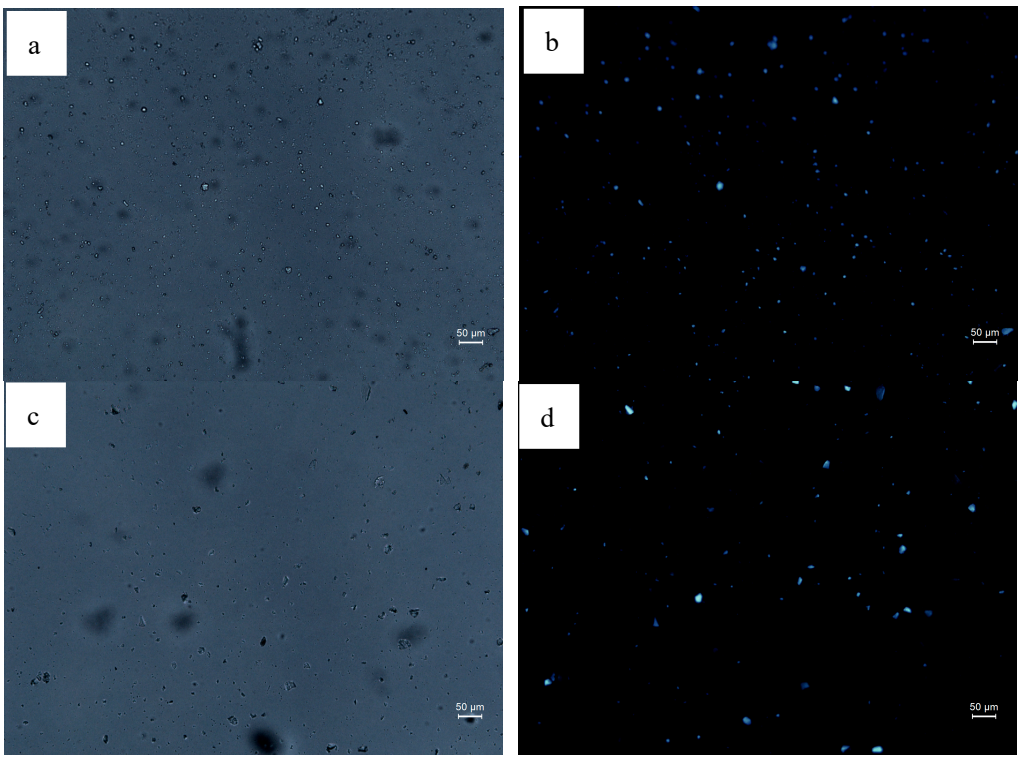

Figure S10. Fluorescence images of the powder of 1 under dark-field (a) and bright-field (b); fluorescence images of **1/PAO10** under dark-field (c) and bright-field (d).

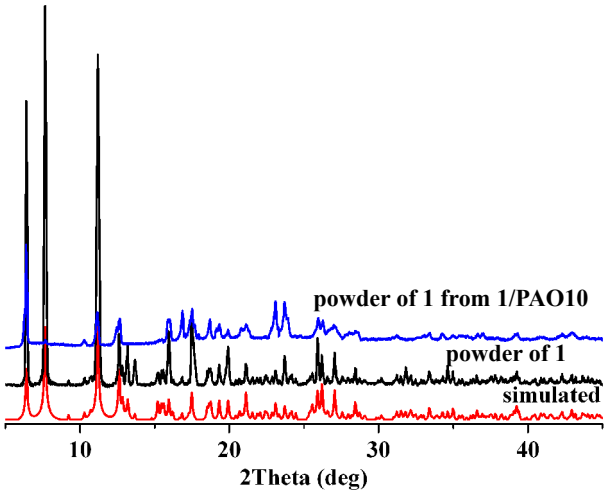

Figure S11. PXRD patterns for **1** [simulated (red), powder (black) and powder from **1/PAO10** (blue)].

Table S1. Reported coordination polymers with $dppa^{4-}$ ligand.

Compound	Coordination mode of H_4dppa	Structure	Properties	Ref.
$[Cd_2(dppa)(H_2O)_5]_n$	μ5- mode IX, Figure S3	3D network	Luninescent property	21
$\{[Cu_3(dppa)_2(\mu\text{-}OH)_2(H_2O)_4]\cdot 2H_2O\}_n$	μ7- mode VI, Figure S3	3D network	Magnetic property	21
$\{[Cd_2(dppa)(4,4\text{-}bipy)_2(H_2O)_3]\cdot 2H_2O\}_n$	μ4- mode X, Figure S3	2D sheet	Luninescent property	21
$[Zn_2(dppa)(4,4\text{-}bipy)_2(H_2O)_3]_n$	μ5- mode VIII, Figure S3	3D network	Luninescent property	21
$\{[Ni_7(dppa)_4(4,4\text{-}bipy)_{12}(H_2O)_{12}]\cdot 2H_2O\}_n$	μ4-/μ3- mode XII/XIII, Figure S3	3D network	Magnetic property	21
$\{[Cu_5(dppa)_2(\mu\text{-}OH)_2(H_2O)_4]\cdot DMF\cdot 10.5H_2O\}_n$	μ7- mode VI, Figure S3	3D network	Catalytic degrades dyes	22
$[Cd_2(dppa)]_n$	μ7- mode IV, Figure S3	3D network	Luninescent property	26
$[Zn_2(dppa)(bpy)]_n$	μ7- mode III, Figure S3	3D network	fluorescent probe	27
$\{[Mn_2(dppa)(phen)_2]\cdot 5H_2O\}_n$	μ5- mode XI, Figure S3	2D sheet	Magnetic property	25
$\{[Zn_2(dppa)(py)]\cdot H_2O\}_n$	μ6- mode V, Figure S3	2D sheet	Luninescent property	25
$[Co_2(dppa)(4,4\text{-}bipy)_2(H_2O)_3]_n$	μ5- mode VIII, Figure S3	3D network	Magnetic property	23
$\{[Co_2(H2dppa)(4,4\text{-}bipy)(H_2O)_4]\cdot 2H_2O\}_n$	μ2- mode VII, Figure S3	3D network	Magnetic property	24

Table S2. Selected bond lengths (Å) and bond angles (°) for compounds **1** and **2**.

		1			
Zn(1)-O(2)	1.907(4)	Zn(1)-O(7)i	1.907(4)	Zn(1)-O(10)	1.947(4)
Zn(1)-N(1)	2.032(4)	Zn(2)-O(3)ii	1.991(4)	Zn(2)-O(8)iii	1.959(4)
Zn(2)-O(10)	1.931(4)	Zn(2)-N(2)iv	2.067(4)		
O(2)-Zn(1)-O(10)	106.97(19)	O(2)-Zn(1)-O(7)i	112.96(18)	O(7)i-Zn(1)-O(10)	105.86(15)
O(2)-Zn(1)-N(1)	118.52(18)	N(1)-Zn(1)-O(10)	113.91(18)	O(7)i-Zn(1)-N(1)	97.85(16)
O(8)iii-Zn(2)-O(10)	123.10(16)	O(3)ii-Zn(2)-O(10)	104.61(16)	O(3)ii-Zn(2)-O(8)iii	114.94(17)
N(2)iv-Zn(2)-O(10)	113.1(2)	O(8)iii-Zn(2)-N(2)iv	100.89(18)	O(3)ii-Zn(2)-N(2)iv	97.35(18)
		2			
Cd(1)-O(2)	2.256(2)	Cd(1)-O(3)i	2.298(2)	Cd(1)-O(7)ii	2.288(3)
Cd(1)-O(8)iii	2.304(2)	Cd(1)-O(9)iii	2.650(2)	Cd(1)-N(1)	2.294(3)
Cd(2)-O(1)iv	2.230(3)	Cd(2)-O(4)	2.215(3)	Cd(2)-O(6)v	2.260(3)
Cd(2)-O(9)v	2.502(2)	Cd(2)-O(9)vi	2.371(2)	Cd(2)-O(10)	2.250(3)
O(7)ii-Cd(1)-O(2)	112.79(10)	N(1)-Cd(1)-O(2)	87.15(10)	O(7)ii-Cd(1)-N(1)	100.27(10)
O(3)i-Cd(1)-O(2)	165.12(11)	O(7)ii-Cd(1)-O(3)i	81.84(11)	O(3)i-Cd(1)-N(1)	87.52(11)
O(8)iii-Cd(1)-O(2)	85.43(10)	O(7)ii-Cd(1)-O(8)iii	140.21(9)	O(8)iii-Cd(1)-N(1)	116.30(10)
O(3)i-Cd(1)-O(8)iii	84.50(10)	O(2)-Cd(1)-O(9)iii	96.97(8)	O(7)ii-Cd(1)-O(9)iii	89.26(9)
N(1)-Cd(1)-O(9)iii	167.28(10)	O(3)i-Cd(1)-O(9)iii	85.50(9)	O(9)iii-Cd(1)-O(8)iii	52.42(8)
O(1)iv-Cd(2)-O(4)	102.64(11)	O(10)-Cd(2)-O(4)	90.74(11)	O(1)iv-Cd(2)-O(10)	83.03(11)
O(6)v-Cd(2)-O(4)	99.35(11)	O(1)iv-Cd(2)-O(6)v	81.08(10)	O(6)v-Cd(2)-O(10)	162.70(11)
O(9)vi-Cd(2)-O(4)	152.90(9)	O(9)vi-Cd(2)-O(1)iv	103.24(10)	O(9)vi-Cd(2)-O(10)	84.54(9)
O(9)vi-Cd(2)-O(6)v	92.47	O(9)v-Cd(2)-O(4)	90.94(9)	O(9)v-Cd(2)-O(1)iv	154.64(9)
O(9)v-Cd(2)-O(10)	118.53(9)	O(9)v-Cd(2)-O(6)v	75.60(8)	O(9)v-Cd(2)-O(9)vi	68.40(9)

Symmetry transformations used to generate equivalent atoms: i: $x - 1/2, -y + 3/2, z - 1/2$; ii: $x - 1, \quad y, z$; iii: $-x + 3/2, y + 1/2, -z + 3/2$; iv: $x + 3/2, -y + 3/2, z + 1/2$ for **1**; i: $-x + 1/2, y + 1/2, -z + 1/2$; ii: $x - 1/2, -y + 3/2, z + 1/2$; iii: $-x + 1/2, y + 1/2, -z - 1/2$; iv: $x + 1/2, -y + 3/2, z + 1/2$; v: $x, y, z + 1$; vi: $-x + 1, -y + 1, -z$.) for **2**.

Table S3. Hydrogen bond lengths (Å) and angles (°) of compound **2**.

D-H···A	*d*(D-H)	*d*(H···A)	*d*(D···A)	∠DHA
O(10)-H(1W)···N(2)i	0.853	1.893	2.728	165.76
O(10)-H(2W)···O(7)i	0.853	2.070	2.757	137.11

Symmetry code: i: $-x+1/2, y+1/2, -z+1/2$.

Table S4 Substrate scope for Zn-catalyzed the Knoevenagel reaction of substituted benzaldehydes with malononitrile [a]

Entry	Substituted benzaldehyde substrate (R-C_6H_4CHO)	Product Yield[b], %
1	R = H	100
2	R = 2-NO_2	100
3	R = 3-NO_2	100
4	R = 4-NO_2	100
5	R = 4-Cl	100
6	R = 4-OH	37
7	R = 4-CH_3	98
8	R = 4-OCH_3	68

[a] Reaction conditions: aldehyde (0.5 mmol), malononitrile (1.0 mmol), catalyst **1** (2.0 mol%), and CH_2Cl_2 (1.0 mL) at 25°C. [b] Calculated by ^{1}H NMR spectroscopy.

Table S5. Comparison of various catalysts for the Knoevenagel condensation reaction between benzaldehyde and propanedinitrile.

Entry	Catalyst	Catalyst (mol%)	Solvent	Time (h)	Temp. (°C)	Conversion (%)	Ref.
1	$[Zn_2(\mu_4\text{-dppa})(\mu\text{-dpe})(\mu\text{-}H_2O)]_n \cdot n H_2O$	2	MeOH	1	RT	100	This work
2	$Zn_3(OH)(ATTCA)_2(H_2O)]\cdot C_2H_6NH_2\cdot 4DMF\cdot H_2O$	10	DCM	5	RT	94	48
3	$[Zn_3(L)_2(\mu_2\text{-}OH)_2]_n$	4	H_2O	8	90	78	49
4	$[Zn_2(TCA)(BIB)_{2.5}]\cdot(NO_3)$	0.3	–	1	60	99	28
5	$\{[Zr_6(\mu_3\text{-}O)_4(\mu_3\text{-}OH)_4(OH)_4(H_2O)_4(DCBA)_2]\cdot 5DMF\cdot 3H_2O\}$	10	DCM	5	RT	89	47
6	$\{[Ba_3Zn_4(TDP)_2(HCO_2)_2(OH_2)_2]\cdot 7DMF\cdot 4H_2O\}_n$	3	Ethanol	1	60	99	44
7	$\{[Zn(L)(bpfp)](H_2O)_3\}_n$	5	DMF	3	35	98	26
8	$[Zn(L)(H_2O)_2]_n \cdot n$(N-methylformamide)]	3	MeOH	1.5	40	75	50
9	$[PbL_2]\cdot 2DMF\cdot 6H_2O$	3	CH_3CN	24	RT	>99	51
10	$[Co_2(tdc)_2(tpxn)]\cdot 6H_2O\}_n$	2	MeOH	1	25-30	96	52
11	$[Zn(L1)(NMeF)]_n \cdot n$(NMeF)	3	H_2O	6	50	>99	53
12	$\{[Cd(Py_2TTz)(2\text{-}NH_2\text{-}BDC)]\cdot(DMF)\cdot 0.5(H_2O)\}_n$	2	–	6	60	99.8	27
13	$[Zn_{15}(mbpz)_6(Hmbpz)_6(L\text{-}NO_2)_4(HL\text{-}NO_2)_2(\mu_3\text{-}OH)_2]_n$	0.6	–	1	80	>99	54

Linkers in coordination polymer catalysts: H_3ATTCA: 2-amino[1,1:3,1-terphenyl]-4,4,5-tricarboxylic acid; H_2L: 2-(hydroxymethyl)-1H-benzo[d]imidazole-5-carboxylic acid; H_3TCA: tricarboxytriphenyl amine, BIB:1,3-bis(imidazol-1-ylmethyl)benzene; H_4DCBA: 4",6'-diamino-5',5"-bis(4-carboxyphenyl)-[1,1':3',1":3",1'"-quaterphenyl]-4,4'"-dicarboxylic acid; H_6TDP: 2,4,6-tri(2,4-dicarboxyphenyl)pyridine; H_2L: methyl-3-hydroxy-5-carboxy-2-thiophenecarboxylate, bpfp: bis(4-pyridylformyl)piperazine;L: 5-acetamidoisophthalic acid; HL: *N*-(4-carboxyphenyl)isonicotinamide 1-oxide;tpxn: N,N'-(1,4-phenylenebis(methylene))bis(1-(pyridin-2-yl)-N-(pyridin-2-ylmethyl)methanamine, H_2tdc: thiophene-2,5-dicarboxylic acid; H_2L1: 5-{(pyren-4-ylmethyl)amino}isophthalic acid; 2-NH_2-H_2BDC: 2-amino-1,4-benzenedicarboxylic acid, Py2TTz: 2,5-bis(4-pyridyl)thiazolo[5,4-d]thiazole; H_2mbpz: 3,3',5,5'-Tetramethyl-4,4'-bi-1H-pyrazole, H_2L-NO_2: 2,2'-Dinitro-[1,1'-biphenyl]-4,4'-dicarboxylic acid.